Available online at www.sciencedirect.com
SCIENCE DIRECT®
Journal of Sound and Vibration 283 (2005) 997–1013
JOURNAL OF SOUND AND VIBRATION
www.elsevier.com/locate/jsvi

Transversal waves in beams via the network simulation method

E. Castro[a], M.T. García-Hernández[a,*], A. Gallego[b]

[a]*Departamento de Física, Escuela Politécnica Superior, Campus Las Lagunillas, Universidad de Jaén, 23071 Jaén, Spain*
[b]*Departamento de Física Aplicada, Escuela Universitaria de Arquitectura Técnica, Universidad de Granada, Granada, Spain*

Received 27 May 2003; received in revised form 29 April 2004; accepted 27 May 2004
Available online 11 November 2004

Abstract

In this paper the Network Simulation Method (NSM) is proposed as a tool for solving the transverse-motion of thin beams resulting from a bending action. The reliability and robustness of the proposed technique is demonstrated with two examples, in which a pinned–pinned beam and a clamped-mass load beam are, respectively, submitted to different flexural forces. The NSM is a numerical technique for the solution of linear and non-linear problems, which are defined by a mathematical model.

Assuming that the electrical variables of voltage and current are equivalent, respectively, to the displacement and the spatial variation of the displacement, a network model for each volume element is designed such that electrical equations are formally equivalent to the spatial discretised equations of the mechanical model. The whole network model, including the devices associated with the boundary conditions, is solved by the numerical computer code PSPICE.

The numerical results have been compared with those obtained by the mode-superposition method: the agreement between them is impressive. The temporal behaviour of each quantity involved in the problem is obtained without transform complications, since the whole study has been conducted in the time-domain, with the possibility of obtaining the corresponding spectral content at the end of calculation. The main contribution of the present paper, therefore, is to employ the NSM numerical method in order to arrive at solutions, in the time-domain, of dynamic mechanical problems. One must also emphasize that NSM has not previously been used by other authors to solve physical problems like the ones presented here.

*Corresponding author. Tel.: +34-953-212377.
E-mail address: tgarcia@ujaen.es (M.T. García-Hernández).

0022-460X/$ - see front matter
doi:10.1016/j.jsv.2004.05.026

1. Introduction

In medical science, material science, engineering or information technology industries, we often need to know the dynamic behaviour of beams submitted to different boundary conditions (as a means, for example, of preventing local deformation, fracture or damage in structures).

The vibration of beams with a variety of boundary conditions has in the last three decades been thoroughly investigated, in both breadth and detail. The normal mode superposition technique is probably the most popular, in which the beam displacement is expressed as a linear combination of eigenfunctions or mode shapes [1–6]. However, we cannot avoid referring other important methods that deal with this kind of problem; we refer here to transform methods such as, among others, the finite Fourier transform [7], the Laplace transform [8–10] or combinations of both of them [11], the finite-difference method [12–16], the Galerkin method [17,18], and the transfer-matrix method [19,20].

In this paper, an approach called the Network Simulation Method (NSM) is proposed as a means of solving the transverse motion of beams resulting from a bending action. The aim of this work is to introduce this method to these kinds of physical problem and demonstrate its reliability and robustness using two examples, in which a pinned–pinned and a clamped-mass load beam are, respectively, submitted to different forces.

The NSM is a numerical technique used to solve linear and non-linear problems, which are defined by a mathematical model. The method has been applied to electrode processes [21,22], membrane processes [23] and heat-transfer processes [24]. Only the spatial variable is discretised and the resulting differential equation, with time as a continuous variable, is used to design the network model. Assuming that the electrical variables of voltage and current are, respectively, equivalent to the displacement and to the spatial variation of the displacement, a network-model for each volume element is designed, in such a way that its electrical equations are formally equivalent to the spatial discretised equation. The whole network-model, including the devices associated with the boundary conditions, is solved by the numerical computer code PSPICE [25].

There are other methods that make use of the analogy between equations and the behaviour of waves and electrical circuits, to study wave-propagation in fluids and solids. Two of the more significant are the Transmission Line Method (TLM) [26,27] and the Digital Waveguide Network (DWN) [28]. Both methods use electrical circuits in the establishment of the guidelines to the techniques. The main differences between these methods and NSM are thus: in TLM and DWN it is necessary to divide the region of interest into a rectangular mesh of transmission lines, where nodes are points of discontinuity for impedance, in this way filling the domain with scattering nodes or junctions. These junctions act as power-conserving signal-processing blocks, and are then linked by transmission-lines. These transmission-lines work with distributed circuit elements. By direct contrast, the circuit elements in NSM are concentrated.

In this paper, the theoretical Euler–Bernoulli model is used for the transverse vibration of beams [1], and the general solution obtained by mode-superposition analysis is compared here with the simulated solution by NSM, to prove the usefulness of this technique in vibration problems. The additional advantage, in the study of such problems, is the obtaining of important quantities, not only in the frequency-domain but in the time domain as well. The main contribution of the present paper, therefore, is the use of the NSM numerical method to find solutions in the time-domain of dynamic mechanical problems like the ones proposed here. In our opinion, the advantages of this method are as follows:

- Its ability, in comparison with other methods, to work in the time-domain with an acceptable computational cost.
- The direct relationship in our mechanical problem between the electrical and physical variables, the latter of which can therefore be easily identified. The vertical displacement, for example, is represented by the voltage; the shear force by the current; and the bending-moment in a circuit model can easily be represented by the second derivative of the voltage.
- The relative simplicity of programming the method using the commercial PSPICE programme, and the fact that time-solution can be performed by this programme as well. The PSPICE is now highly developed, and can thus be used to deduce the dynamic behaviour of the system directly from the graph without having to deal explicitly with the differential equations.
- The method is not limited by the complexity of the system's processes, and allows extremely complicated mathemetical problems to be solved by an efficient graphical method at a very reasonable cost.

As for the disadvantages of this numerical method, they occurred to us as follows:

- The programmer must be well acquainted with the conventional circuit theory. If not, it will be difficult accurately to write down the circuits simulating the mechanical problem.
- The inherent limitations of the PSPICE programme, both in terms of time discretization and frequency.

2. The mathematical model

The problem considered is the transversal vibration of an uniform elastic beam of finite length L, originally at rest, with classical boundary-conditions at $x^*=0$ and L, the Euler–Bernoulli model has been selected to study it [1].

Denoting y^* as the displacement or deflection in the beam, in which x^* represents the position and t^* the time, the familiar governing equation of the beam is [1]:

$$\frac{\partial^4 y^*(x^*,t^*)}{\partial x^{*4}} + \frac{1}{a^2}\frac{\partial^2 y^*(x^*,t^*)}{\partial t^{*2}} = 0, \tag{1}$$

where a is a parameter that depends on the physical characteristics of the beam, $a^2=EI/(\rho S)$, E being the Young modulus, I the area inertia moment, ρ the density, and S the cross-sectional area of the beam.

Sundry boundary conditions have been simulated with NSM, with good results, but two particular cases are presented here: a beam both in pinned–pinned and clamped-mass load boundary conditions, with both in forced vibration situations, such as a pulse and a harmonic force applied to any point of the beam.

For the case in which a pinned–pinned beam is considered, the boundary conditions are given by

$$y^*(0,t^*) = y^*(L,t^*) = 0, \tag{2}$$

$$\frac{\partial^2 y^*(0,t^*)}{\partial x^{*2}} = \frac{\partial^2 y^*(L,t^*)}{\partial x^{*2}} = 0. \tag{3}$$

For a clamped-mass load, the boundary conditions are

$$y^*(0,t^*) = \frac{\partial y^*(0,t^*)}{\partial x^*} = 0, \tag{4}$$

$$\frac{\partial^2 y^*(L,t^*)}{\partial x^{*2}} = 0, \tag{5}$$

$$EI\frac{\partial^3 y^*(L,t^*)}{\partial x^{*3}} = m\frac{\partial^2 y^*(L,t^*)}{\partial t^{*2}}, \tag{6}$$

where m is the mass of the load at $x^* = L$.

As mentioned above, two different types of force are used in this paper. First, a step-pulse $F(x^*,t^*)$ is applied at the point $x_0{}^*$

$$F(x^*,t^*) = \delta(x^* - x_0^*)H(t^* - t_0^*), \tag{7}$$

where $\delta(x^*)$ is the Dirac delta function and $H(t^*)$ is the Heaviside function. As a second case, it has been considered that a harmonic force is applied at the point $x_0{}^*$

$$F(x^*,t^*) = \delta(x^* - x_0^*)\sin(\omega_a^* t^*), \tag{8}$$

where ω_a^* is the frequency of the applied force.

Once the mechanical mathematical model with boundary conditions has been established, we will consider the problem of obtaining the network model for the situations described here.

3. Network model

The network-model can be considered as another representation of the physical process. As it is outlined below, the network is equivalent to the differential equation of motion, except for the approximations it is necessary to make.

The equation of the motion of the flexural vibrations of a beam, in the Euler–Bernoulli model, is the transversal wave equation given by Eq. (1). It is convenient to write down this equation in a dimensionless form, so that the obtained results can be more general and useful. If L is the length of the beam, the dimensionless variables are defined as

$$x = x^*/L, \quad y = y^*/L, \quad t = at^*/L^2, \quad \omega_a = L^2\omega_a^*/a. \tag{9}$$

Thus, the transversal wave equation (1) becomes

$$\frac{\partial^4 y}{\partial x^4} + \frac{\partial^2 y}{\partial t^2} = 0. \tag{10}$$

The NSM works with two variables, a scalar-variable that is treated as a voltage, and a vectorial-variable that is treated as a current. In this case, it is possible to choose the scalar-variable as the vertical displacement. However, as this method has not been applied in previous work to these kinds of partial differential equation, it is not clear which vectorial-variable can be considered to be the current. In previous applications of the NSM to other physical processes, the current has always been connected with $(\partial y/\partial x)$, but there are no physical quantities related to it here. The important quantities of the flexural vibrations, apart from the vertical displacement, are the bending moment and the shear force, which are connected, respectively, with the second and third spatial derivative of the displacement. We have found that the application of the NSM to the transversal vibrations of a beam requires the definition of the current as the third spatial derivative of the displacement, so that it can be related with the shear force. Thus, the current is defined as

$$j \equiv \frac{\partial^3 y}{\partial x^3}. \tag{11}$$

With this definition of the current, the transversal wave equation given by Eq. (10) can be written in the following form:

$$\frac{\partial j}{\partial x} + \frac{\partial^2 y}{\partial t^2} = 0. \tag{12}$$

This is a partial differential equation with two variables, y and j. With a spatial discretization of the dimensionless beam in N cells of length $\Delta x = 1/N$, this partial differential equation can be transformed into a system of connected differential equations, given by

$$\frac{j_{i+\Delta} - j_{i-\Delta}}{\Delta x} + \left(\frac{d^2 y_i}{dt^2}\right) = 0; \qquad i = 1, 2, \ldots, N, \tag{13}$$

where $j_{i+\Delta}$ is the current to the right of the cell i, $j_{i-\Delta}$ is the current to the left of it, and y_i is the vertical displacement in the middle of cell i. This is the governing equation of the vertical displacement in this cell.

Operating on Eq. (13), it becomes

$$j_{i+\Delta} - j_{i-\Delta} + \Delta x \left(\frac{d^2 y_i}{dt^2}\right) = 0. \tag{14}$$

In this equation there are two currents, $j_{i+\Delta}$ and $j_{i-\Delta}$, and a third term which can be treated as a current too. It can be more clearly understood with the following definition of $j_{\gamma i}$:

$$j_{\gamma i} \equiv \Delta x \left(\frac{d^2 y_i}{dt^2}\right) \tag{15}$$

Eq. (14) is then transformed into

$$j_{i-\Delta} - j_{i+\Delta} - j_{\gamma i} = 0. \tag{16}$$

Therefore, the governing equation of the cell i can be represented as the balance of the currents that enter and leave the cell. It can be demonstrated that $j_{i-\Delta} = j_{(i-1)+\Delta}$ and $j_{i+\Delta} = j_{(i+1)-\Delta}$. Thus, adjacent cells are connected by these currents: this fact is shown by Fig. 1. Taking this result into account, Eq. (16) is represented by the circuit in Fig. 2. This figure shows the balance of currents for cell i, but the values are not yet known. Thus, auxiliary circuits are necessary to obtain

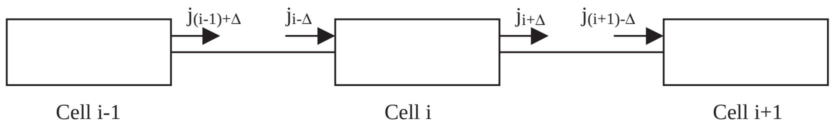

Fig. 1. Scheme of cells and currents.

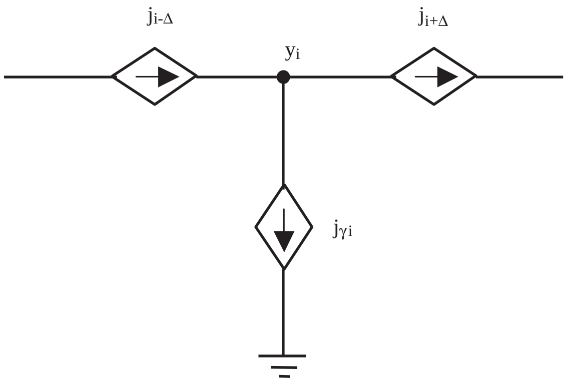

Fig. 2. Basic cell of the network model without auxiliary circuits.

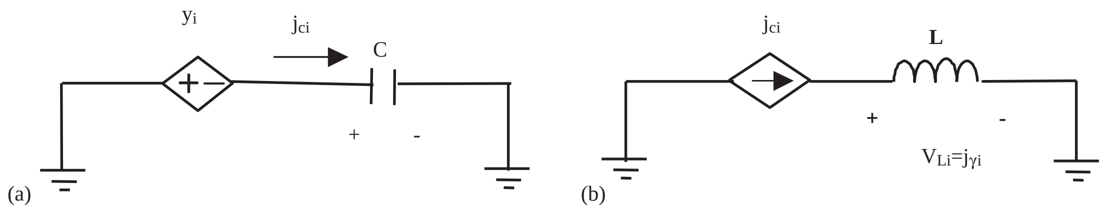

Fig. 3. Auxiliary circuits of the basic cell to obtain $j_{\gamma i}$ of Fig. 2.

numerical values for those currents. These auxiliary circuits are specific for each current, and are the circuit representation of the mathematical expression of the currents.

Fig. 3 shows two auxiliary currents needed to model the current $j_{\gamma i}$ defined by the Eq. (15). In the second of them (Fig. 3b) there is a current source whose value is j_{ci} and an inductor L. Taking into account the circuit theory, the following equation can be written for this circuit:

$$V_{Li} = L\frac{\mathrm{d}j_{ci}}{\mathrm{d}t}. \tag{17}$$

In particular, by making the value of V_{Li} equal to the current value $j_{\gamma i}$ (i.e. $V_{Li} \equiv j_{\gamma i}$), we find that

$$j_{\gamma i} = L\frac{\mathrm{d}j_{ci}}{\mathrm{d}t}. \tag{18}$$

On the other hand, in Fig. 3a there is a circuit with a voltage source whose value is y_i (the vertical displacement in cell i) and a capacitor C, in which the current must be equal to j_{ci} (the current in

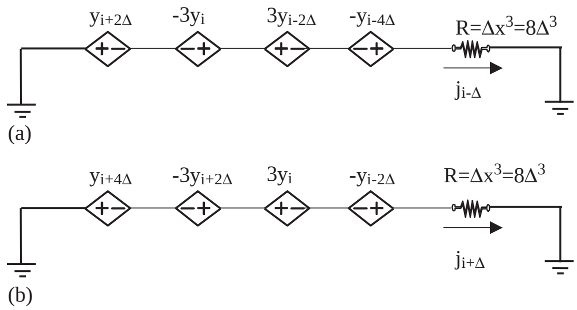

Fig. 4. Auxiliary circuits to obtain $j_{i-\Delta}$ and $j_{i+\Delta}$ of Fig. 2.

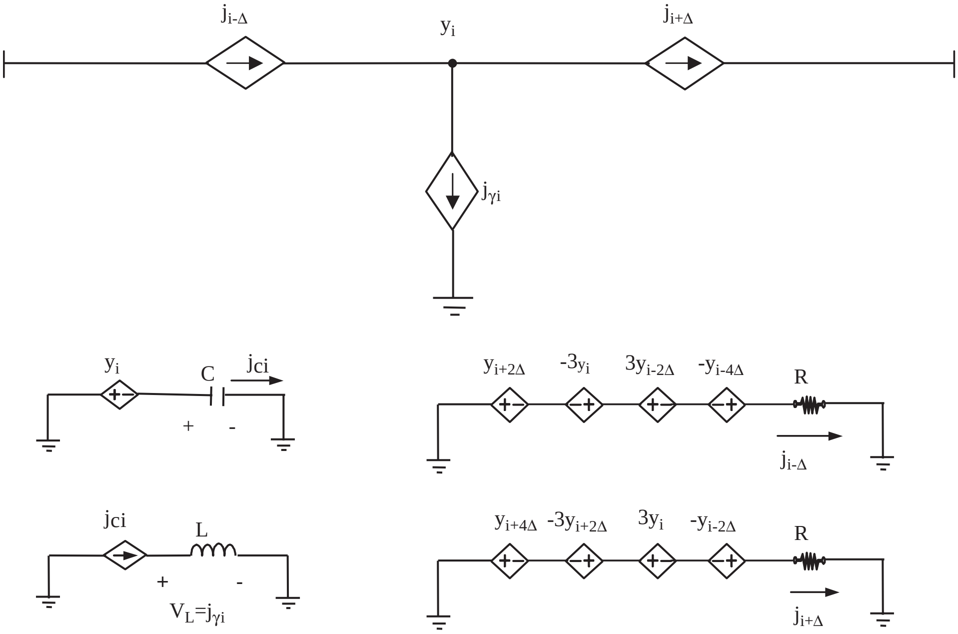

Fig. 5. Basic cell with all auxiliary circuits.

the circuit of Fig. 3b). If we use the circuit theory, we have it thus:

$$j_{ci} = C\frac{\mathrm{d}y_i}{\mathrm{d}t} \;\Rightarrow\; \frac{\mathrm{d}j_{ci}}{\mathrm{d}t} = C\frac{\mathrm{d}^2 y_i}{\mathrm{d}t^2}. \tag{19}$$

Taking account of Eqs. (18) and (19), the following relationship between y_i and $j_{\gamma i}$ is found:

$$j_{\gamma i} = LC\frac{\mathrm{d}^2 y_i}{\mathrm{d}t^2}. \tag{20}$$

This, by choosing $LC = \Delta x$, is exactly equivalent to Eq. (15). We can thus obtain the current $j_{\gamma i}$ through the auxiliary circuits in Fig. 3, with $LC = \Delta x$ being the equivalent of the electrical components (L and C) with the system parameter Δx. If we use Eq. (1) instead of the dimensionless equation (10) in the design of the network model, LC has to be equal to $a^2\Delta x$, these circuit parameters being related to the physical characteristics of the beam.

The auxiliary circuits that provide the currents $j_{i\pm\Delta}$ are shown in Fig. 4. These circuits are based on the following finite-difference approximation:

$$\frac{\partial^3 y}{\partial x^3} \approx \frac{y_{i+3\Delta} - 3y_{i+\Delta} + 3y_{i-\Delta} - y_{i-3\Delta}}{8\Delta^3}. \tag{21}$$

All these circuits (Figs. 2–4) form the basic cell in th e network-model for the flexural vibrations of a beam, as can be seen in Fig. 5. The complete network model is formed by the connection of N of these basic cells and the incorporation of the boundary conditions at each end of the network.

4. Boundary conditions

The selection of the boundary-conditions has been carried out by designing a circuit that produces the same effect on the network-model as that which the boundary conditions produce on the vibrating beam. Thus it is necessary to implement a circuit with the same mathematical expression as the boundary end condition. The circuits of the ends of the network model, for the two cases considered in this paper, are developed in this section.

4.1. Pinned–pinned beam

The end conditions of a simply supported beam, expressed with dimensionless variables, are given by

$$y(0,t) = y(1,t) = 0, \tag{22}$$

$$\left(\frac{\partial^2 y}{\partial x^2}\right)_{0,t} = \left(\frac{\partial^2 y}{\partial x^2}\right)_{1,t} = 0. \tag{23}$$

The first condition is implemented in the network model by earthing the nodes $i=0$, N, corresponding to $x=0$, 1. The second condition can be incorporated by approximating the spatial second derivative using the finite-difference

$$\frac{\partial^2 y}{\partial x^2} = \frac{y_{i+1} - 2y_i + y_{i-1}}{\Delta x^2} \tag{24}$$

and adapting the first and last basic cells to this relationship between the variables, as shown in Fig. 6.

4.2. Clamped–mass load beam

The end conditions for this case are

$$\text{Clamped:} \quad y(0,t) = \left(\frac{\partial y}{\partial x}\right)_{0,t} = 0, \tag{25}$$

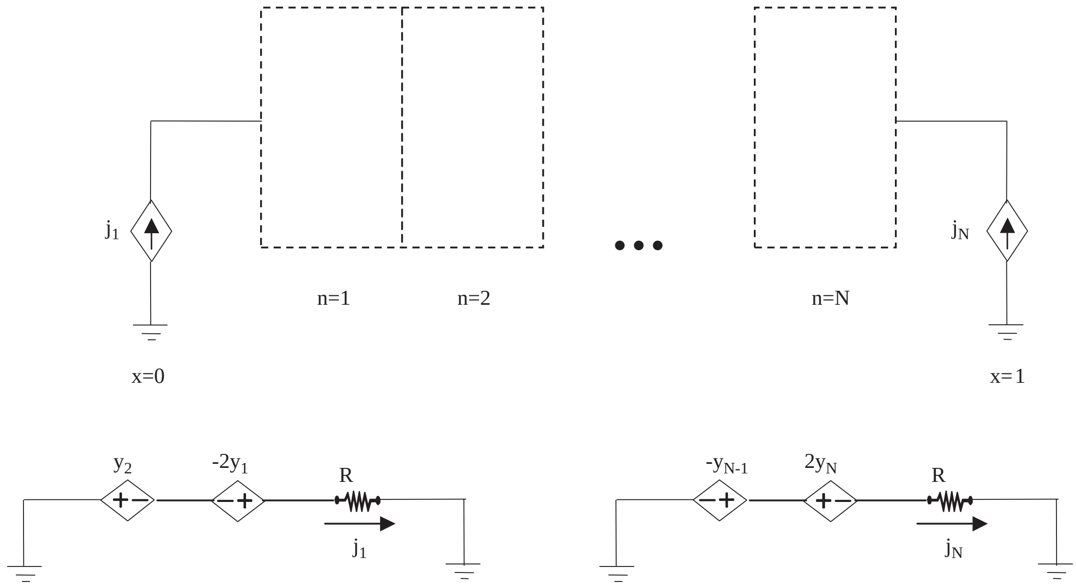

Fig. 6. Complete network model of the pinned–pinned beam.

$$\text{Mass load:} \quad \left(\frac{\partial^2 y}{\partial x^2}\right)_1 = 0, \tag{26}$$

$$\left(\frac{\partial^3 y}{\partial x^3}\right)_{1,t} = m_a \left(\frac{\partial^2 y}{\partial t^2}\right)_{1,t}, \tag{27}$$

where $m_a = m/M$ is a parameter dependent on the ratio between the attached mass m and the mass of the beam M. The clamped conditions are implemented by earthing the node $i = N$ and approximating the spatial first derivative using its finite differences:

$$\left(\frac{\partial y}{\partial x}\right) = \frac{y_{i+1} - y_{i-1}}{2\Delta x}. \tag{28}$$

The first condition, (26), of the mass-load-end is again approximated using its finite-differences. However, to incorporate the second condition, (27), it is necessary to implement a current source controlled by an auxiliary circuit (Fig. 7), where $C_m L_m = m_a$. The current j_m can be considered equivalent to the inertial force applied to the beam by the tip-mass, while the auxiliary circuits determining it are equivalent to the acceleration of the mass-load (Fig. 7).

5. Simulation and results

5.1. Pinned–pinned beam

In the case of a pinned–pinned beam, the transversal wave equation can be solved theoretically, using the eigenfunctions of this kind of beam. It can thus be used to test the effectiveness of

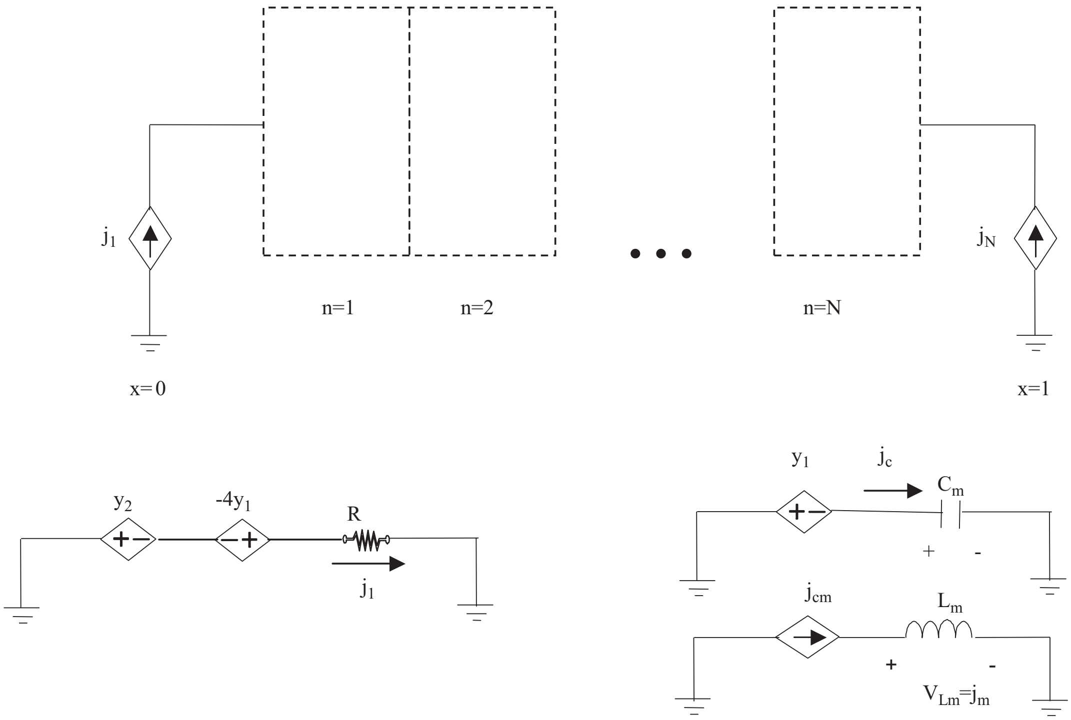

Fig. 7. Complete network model of the clamped-mass load beam.

applying NSM to this problem. In order to check it more efficiently, the application of two different forces has been considered: a step-pulse and a harmonic force. The application of the step pulse in two different positions of the beam has been considered as well. Thus, the flexural vibration of a pinned–pinned beam has been simulated in three different situations: when the step-pulse is applied in the middle of the beam ($x=1/2$); when it is applied at $x=1/3$; and when a harmonic force of frequency $f=\pi$ is applied to the middle of the beam. The choice of this frequency for the harmonic force is due to the fact that the eigenfrequencies of the pinned beam are $f_n = n^2\pi/2$, $n=1, 2, 3,$...etc. Hence, in our case the first eigenfrequency is $\pi/2$ and the second is 2π. The frequency of the harmonic force is therefore of the same order as the eigenfrequencies of the beam. As demonstrated in Section 2, the step-pulse has the form given in Eq. (7). For this particular case, we have that $t=0.05$ and $x=0.5$ or 0.33. The period of the first eigenfrequency is $t=0.64$. By comparing it with the duration of the step-pulse, it is possible to obtain a difference of one order of magnitude. Thus, $F(x,t)$ can be considered as an impulsive pulse.

In all the cases the values of the circuit parameters are conditioned by N. Choosing $N=150$, we find that $C=L=0.08165$ and $R=0.0005443$. With these respective values for the parameters, the two simulations have been conducted. Fig. 8 shows the comparison between the simulation results for the vertical displacement and analytical solution when the step-pulse is applied at the mid-point of the beam: we can see here that the theoretical and simulation results are almost identical. Fig. 9 shows the comparison between the bending moment obtained from simulation work and

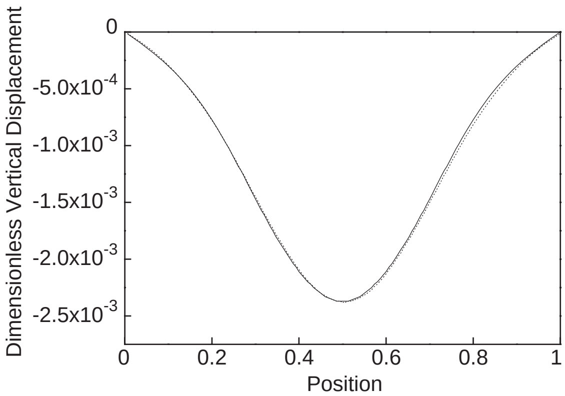

Fig. 8. Comparison between the simulation results and the analytical solution along the beam for displacement in $t = 1$, when the step pulse is applied at $x = 0.5$. —— Simulation results; ··· ··· ···Analytical solution.

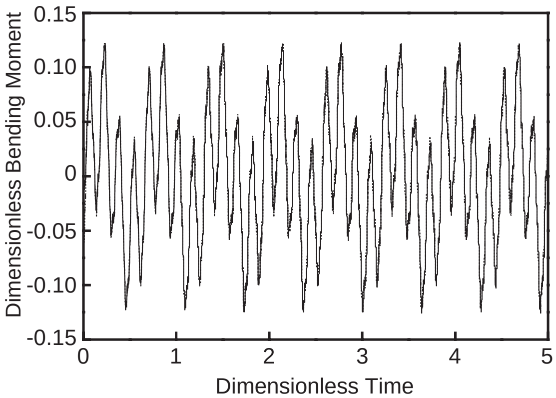

Fig. 9. Comparison between the simulation results and the analytical solution at $x = 0.2$ for bending moment, when the step pulse is applied at $x = 0.33$. —— Simulation results; ··· ··· ··· Analytical solution.

the analytical one versus time at $x = 0.2$ when the step-pulse is applied at $x = 0.33$. In this case the motion is complicated but with a cyclical form, and the simulation gives results very similar to the analytical ones.

The harmonic force is given by Eq. (8), where the parameter values are $x_0 = 0.5$ and $\omega_a = 2\pi^2$. Figs. 10 and 11 show, respectively, the comparison between the vertical displacement and the shear force, these data being obtained from the simulation and analytical work at two points of the beam, when the excitation is the harmonic force. It is therefore possible to conclude that the NSM works successfully in both of the simulated cases. An error diagram is shown in Fig. 12 for the discrepancy between the simulation results, for the displacement at $x = 0.2$, with the excitation a harmonic force. It can be seen that most of the time the margin of error is very slight, and invariably less than 1%. For the sake of brevity, we have only included one error diagram: however, the same was true for all the simulated cases.

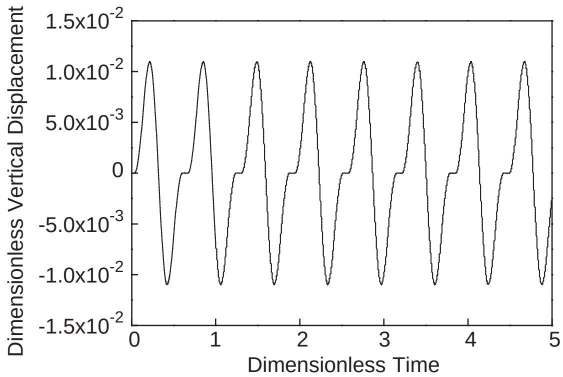

Fig. 10. Comparison between the simulation results for the displacement and the analytical solution at $x = 0.2$, when the harmonic force ($\omega_a = 2\pi^2$) is applied at $x_0 = 0.5$. —— Simulation results; $\cdots$ $\cdots$ $\cdots$ Analytical solution.

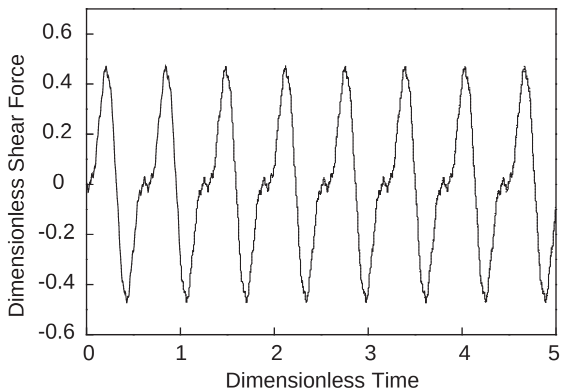

Fig. 11. Comparison between the simulation results for the shear force and the analytical solution at $x = 0.8$, when the harmonic force ($\omega_a = 2\pi^2$) is applied at $x_0 = 0.5$. —— Simulation results; $\cdots$ $\cdots$ $\cdots$Analytical solution.

5.2. Clamped-mass load beam

Consider now a beam clamped at $x = 0$ with a concentrated mass at the abscissa $x = 1$. Once again, two different types of excitation-force have been applied to the beam. First to be carried out was the study of the beam with a pulse applied to its mid-point, to assess the behaviour of some of the system's major quantities, like displacement or shear force. Next, a case was conducted in which a beam was excited by means of a harmonic force.

In neither situation it is possible to obtain analytical solutions by the mode superposition method [29]. Therefore, in the present section of this paper, only results of simulations using NSM are presented, with the exception of a comparison of the natural frequencies obtained with other methods.

First, we considered a step-pulse applied in the middle of the beam. The parameter values were the same as in Section 5.1. Fig. 13 shows different aspects of the response of the beam to the

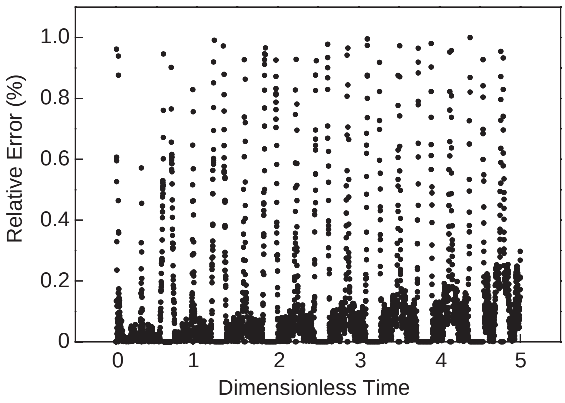

Fig. 12. Relative error of the simulation results for the displacement at $x = 0.2$ shown in Fig. 10.

step-pulse. In Fig. 13a, the vertical displacement of the mass load is given versus time. It consists of a cyclical movement formed basically by the first two eigenfrequencies of the beam. In Fig. 13b, the shear force is presented at a point near where the step-pulse is applied. As this step-pulse is very short, the variations of the shear force are extremely fast, and high frequencies appear (much higher than those corresponding to the displacement). We therefore have two variables of the same physical process that fluctuate in a very different way (one of them changing must faster than the other); the NSM, moreover, can handle them at the same time. In Fig. 13c, the variation of the vertical displacement is shown against position at several points. Needless to say, given that the boundary conditions at each end are different, it can be noted that the movement is not symmetrical. The curve at the left end shows the features of a fixed end, with its displacement and slope at zero, while at the right end, although the displacement and slope are not fixed, there is in that zone no curvature. The boundary conditions are, thus, well modelled by NSM. It may be noted that the maximum displacement is not fixed at any particular position—indeed, it changes for each time and can be positioned anywhere between the left-hand end and the middle of the beam, or between the middle and the right-hand end. Its behaviour is not, therefore, as simple as when the pulse is applied at $x = 0.5$ in the pinned–pinned beam, which always has the maximum displacement at its mid-point. Finally, in Fig. 13d, where the variation of the shear force is shown versus position at several times (the same ones as in Fig. 13c), it can be observed that this variation has no regular form and that the waveform changes at each time. This is due to the fact that the variation with time is very complex, and that the load mass produces a shear force at $x = 1$, making the distribution of force neither simple nor symmetrical.

The only theoretical information that we have for this case on the solution of the transversal wave equation is constituted by the natural wave numbers, which are given by the roots of the following equation [30]:

$$\left[1 + \cos(\beta_n)\cosh(\beta_n)\right] = m_a \ \beta_n \ \left[\sin(\beta_n)\cosh(\beta_n) - \cos(\beta_n)\sinh(\beta_n)\right], \tag{29}$$

where $\beta_n = (\omega_n)^{1/2}$ is the dimensionless wave number and ω_n is the dimensionless radial natural frequency. To ensure that the network model used to simulate the behaviour of this beam is correct and appropriate, the roots of Eq. (29) have been compared in Table 1 with the wave

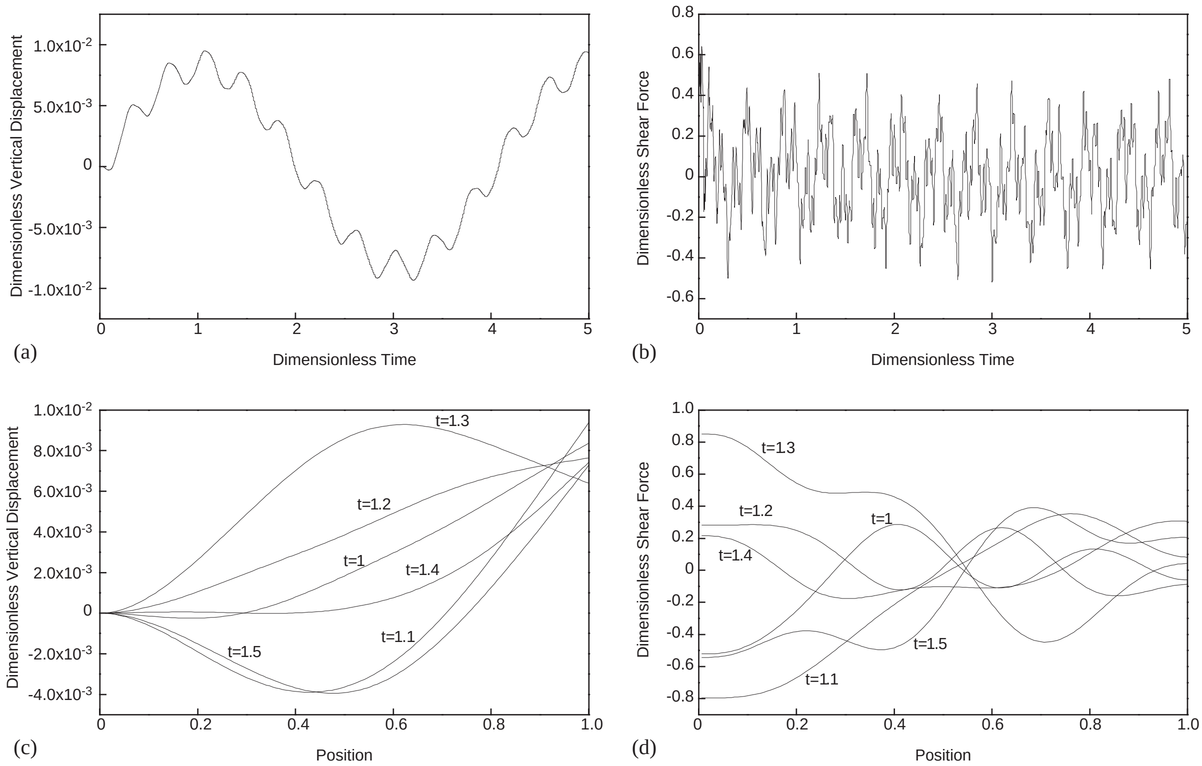

Fig. 13. Response of the clamped-mass load beam to the application of the step pulse at $x = 0.5$. (a) Vertical displacement of the mass load. (b) Shear force at $x = 0.503$. (c) Vertical displacement along the beam in several times. (d) Shear force along the beam in several times.

Table 1
Comparison between the transversal wave numbers obtained from the Fourier Transform of the simulation and the analytical ones

Frequency (dimensionless)	Wave number from simulation (dimensionless)	Theoretical wave number (dimensionless)	Relative error (%)
0.24	1.24	1.25	0.78
2.69	4.11	4.03	1.99
8.05	7.11	7.13	0.31
16.85	10.29	10.26	0.32
28.56	13.40	13.39	0.06
43.21	16.48	16.52	0.28

numbers obtained from the Fourier Transform of the simulated vertical displacement, when the step-pulse is applied. This comparison demonstrates that the wave numbers from the simulation are very similar to the roots of Eq. (29); it can therefore be concluded that the network model is correct.

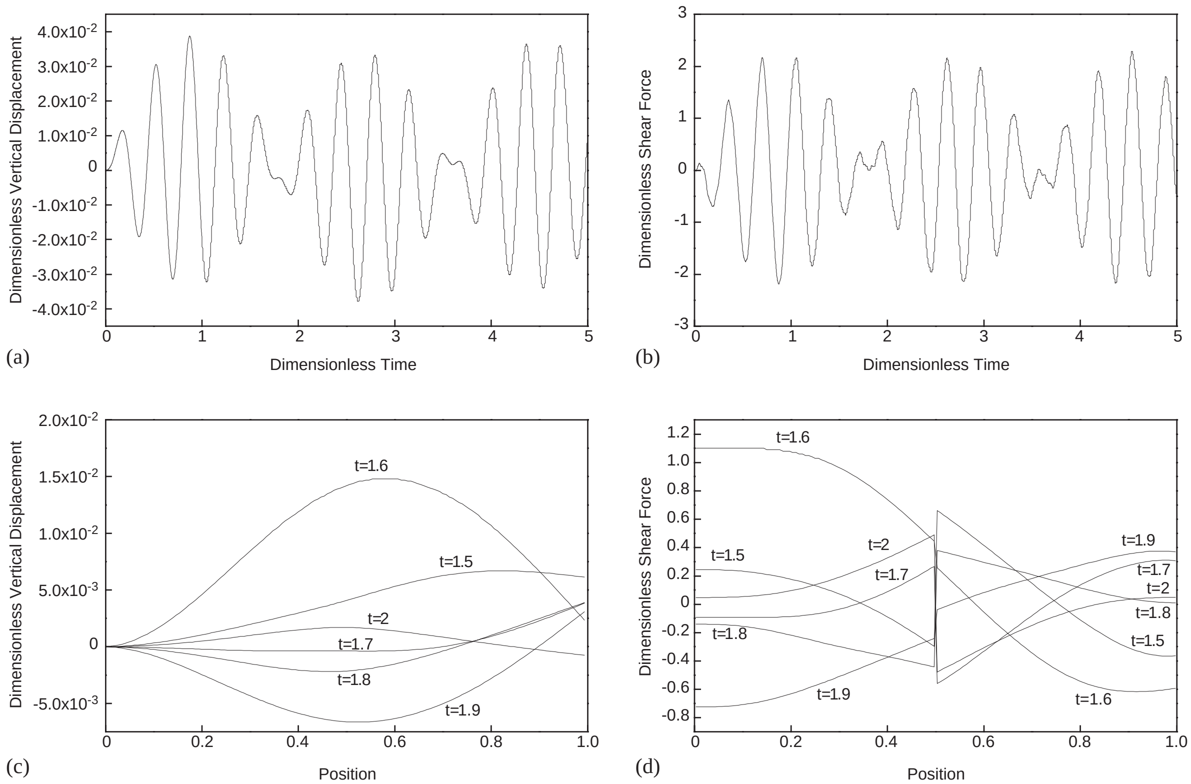

Fig. 14. Response of the clamped-mass load beam to the application of the harmonic force at $x = 0.5$. (a) Vertical displacement in the middle of the beam. (b) Shear force of the mass load. (c) Vertical displacement along the beam in several times. (d) Shear force along the beam in several times.

Finally, there are the results when a harmonic force is applied. In Fig. 14 there are several graphs with different aspects of the response of the clamped-mass load beam to a harmonic force of frequency $\omega_a = 2\pi^2$. In Fig. 14a the vertical displacement is presented in the position where the force is applied, and it is not a simple harmonic movement. In Fig. 14c we have the variation of the displacement versus the position at several times. It can be seen that the wave shapes are similar to those of Fig. 13c, due to the fact that because the force is applied in the same position, the same normal modes are excited. The shear force at the right-hand end of the beam produced by the load-mass can be seen in Fig. 14b. It is a smooth curve (compared with Fig. 13b) similar to Fig. 14a, which is clearly made up of the overlapping of a few harmonic functions whose frequencies are the lower natural frequencies of the beam, together with the excitation frequency. Finally, Fig. 14d shows the variation of the shear force with the position at different times. The main characteristic here is the discontinuity at $x = 0.5$ due to the application at this point of the harmonic force (a localised force applied to the beam produces a discontinuity of the shear force). The form of the shear force is similar to that which appears in other kinds of beam (for example, the pinned–pinned beam) when a harmonic force is applied in the mid-point, including the area of discontinuity. In other cases the shear force at $x = 0.5$ is zero, while in this beam its value is not fixed and changes with time; equally, the distribution of force is, obviously, not symmetrical.

6. Conclusions

In this paper, the Network Simulation Method (NSM) has been used to solve the transverse motion of thin beams originated in a bending action. It has been demonstrated to give efficient and accurate solutions with several boundary conditions. The numerical results have been compared with those obtained by analytical methods, and the agreement is impressive.

An exclusive reliance on the frequency domain is not convenient because frequency techniques are generally less flexible than time techniques; it is, however, also true that many problems are much more easily dealt with in the frequency domain. In this work, the temporal behaviour of each quantity involved has been obtained without transform complications, because the whole study has been carried out in the time-domain, with the possibility of arriving at each spectral dependence at the end of the calculation. This is one of NSM's main advantages.

References

[1] K.F. Graff, *Wave Motion in Elastic Solids*, Dover, New York, 1991.
[2] H.V. Vu, A.M. Ordóñez, B.H. Karnopp, Vibration of a double beam system, *Journal of Sound and Vibration* 229 (2000) 807–822.
[3] M. Gürgöze, A note on the vibrations of restrained beams on rods with point masses, *Journal of Sound and Vibration* 96 (1984) 461–468.
[4] J.S. Wu, T.L. Lin, Free vibration analysis of a uniform cantilever beam with point masses by an analytical and numerical combined method, *Journal of Sound and Vibration* 136 (1990) 201–213.
[5] S. Naguleswaran, Transverse vibrations of an Euler–Bernoulli uniform beam carrying several particles, *International Journal of Mechanical Sciences* 44 (2002) 2463–2478.
[6] M. Gürgöze, On the eigenfrequencies of a cantilever beam with attached tip mass and a spring–mass system, *Journal of Sound and Vibration* 190 (1996) 149–162.
[7] L. Sun, A closed form solution of a Bernoulli-Euler beam on a viscoelastic foundation under harmonic line loads, *Journal of Sound and Vibration* 242 (2001) 619–627.
[8] W.H. Liu, J.R. Wu, C.C. Huang, Free vibration of beams with elastically restrained edges and intermediate concentrated masses, *Journal of Sound and Vibration* 122 (1988) 193–207.
[9] T.P. Chang, F.I. Chang, M.F. Liu, On the eigenvalues of a viscously damped simple beam carrying point masses and springs, *Journal of Sound and Vibration* 240 (2001) 769–778.
[10] R.R. Hamada, H. Nakayama, K. Hayashi, Free and forced vibration of elastically connected double-beam system, *Bulletin of the Japan Society of Mechanical Engineers* (1983) 1936–1942.
[11] W.L. Li, Free Vibration of beams with general boundary conditions, *Journal of Sound and Vibration* 237 (2000) 709–725.
[12] M.G. Salvadori, Numerical computation of buckling loads by finite differences, *Transactions of the American Society of Civil Engineers* 2441 (1994) 590–624.
[13] W. Carnegie, J. Thomas, Effects of shear deformation and rotary inertia on lateral frequencies of cantilever beams in bending, *Journal of Engineering for Industry* 94 (1972) 267.
[14] K.B. Subrahmanyam, A.W. Leissa, An improved finite difference analysis of uncoupled vibrations of cantilever beams, *Journal of Sound and Vibration* 98 (1985) 1–11.
[15] K.B. Subrahmanyam, K.R.V. Kaza, Vibration and bucking of rotating pretwisted, preconed beams including Coriolis effects, *Journal of Vibration, Acoustics, Stress and Reliability in Design* 108 (1986) 140–149.
[16] X.M. Zhang, M. Fatemi, R.R. Kinnick, J.F. Greenleaf, A model for vibration transmission of light-heavy structures connected double-beam systems, *Applied Acoustics* 64 (2003) 213–227.
[17] H. Leipholz, Use of Galerkin's method for vibration problems, *Shock and Vibration Digest* 8 (1976) 3.

[18] K.B. Subrahmanyam, K.R. Kaza, Non-linear flap-lag extensional vibration of rotating pretwisted, preconed beams including Coriolis effects, *International Journal of Mechanical Sciences* 29 (1987) 29–43.
[19] K.B. Subrahmanyam, A.K. Garg, Uncoupled flexural vibrations of straight beams with all possible boundary conditions treated by a transfer matrix method, *Journal of Sound and Vibration* 207 (1997) 397–419.
[20] C.N. Bapat, C. Bapat, Natural frequencies of a beam with non-classical boundary conditions and concentrated masses, *Journal of Sound and Vibration* 112 (1987) 177–182.
[21] M.T. García-Hernández, J. Castilla, C.F. González-Fernández, J. Horno, Application of the network method to simulation of a square scheme with Butler–Volmer charge transfer, *Journal of Electroanalytical Chemistry* 424 (1997) 207–212.
[22] A.J. Bard, I. Rubinstein (Eds.), *Electroanalytical Chemistry*, vol. 19, Marcel Dekker, New York, 1999, pp. 64–68.
[23] J. Castilla, M.T. García-Hernández, A. Hayas, J. Horno, Simulation of non-stationary electrodiffusion processes in charged membranes by the network approach, *Journal of Membrane Science* 116 (1996) 107–116.
[24] F. Alhama, J.F. López-Sánchez, C.F. González-Fernández, Heat conduction through a multilayered wall with variable boundary conditions, *Energy* 228 (1997) 797–803.
[25] *PSPICE, version 80*, Microsim Corporation.
[26] R. Ciocan, N. Ida, Applications of transmission line matrix method for NDT; *NDT.net* 8 (3) (2003).
[27] J.A. Porti, J.A. Morente, A three-dimensional symmetrical condensed TLM node for acoustics, *Journal of Sound and Vibration* 241 (2) (2001) 207–222.
[28] S.D. Bilbao, Wave and Scattering Methods for the Numerical Integration of Partial Differential Equations. PhD. Thesis, Stanford University, May 2001.
[29] S.H. Han, H. Benaroya, T. Wei, Dynamics of transversely vibrating beams using four engineering theories, *Journal of Sound and Vibration* 225 (5) (1999) 935–988.
[30] P. Laura, J.L. Pombo, E.A. Susemihl, Note on vibrations of a clamped–free beam with a tip mass at free end, *Journal of Sound and Vibration* 37 (2) (1974) 161–168.